Open access • Journal Article • DOI:10.1103/PHYSREVA.57.1286

Feedback control of laser intensity noise — Source link

Ben C. Buchler, Elanor H. Huntington, Charles C. Harb, Timothy C. Ralph

Institutions: Australian National University

Published on: 01 Feb 1998 - Physical Review A (American Physical Society)

Topics: Relative intensity noise, Quantum noise, Noise (radio), Laser and Squeezed coherent state

Feedback control of laser intensity noise

Ben C. Buchler, Elanor H. Huntington, Charles C. Harb, and Timothy C. Ralph
Department of Physics, Faculty of Science, The Australian National University, Canberra, Australian Capital Territory 0200, Australia
(Received 13 March 1997)

A fully quantum-mechanical model of feedback to the pump source of a four-level laser is developed with a view to predicting the achievable intensity noise reduction. For solid-state lasers, the model shows that quantum noise sources due to laser dynamics have a significant impact on the optimization of the feedback loop. Experimental results obtained with a diode pumped neodymium:yttrium aluminum garnet (Nd:YAG) laser are found to be in good agreement with the theoretical model. The ultimate limit to the noise suppression comes from the quantum noise due to the measurement processes in the feedback loop. A scheme to overcome this limit using a squeezed vacuum is theoretically demonstrated to be a highly efficient method of generating bright intensity squeezed light, particularly in the kHz regime where bright squeezing is otherwise difficult to obtain. [S1050-2947(97)08111-0]

PACS number(s): 42.60.Mi, 42.50.Lc, 42.50.Dv

I. INTRODUCTION

Numerous applications, for example ultrahigh sensitivity metrology and gravitational wave interferometers, require lasers with low-intensity noise to maximize the signal-to-noise ratio. The standard limit to laser intensity noise is the quantum noise limit (QNL) which corresponds to stochastic fluctuations in the photon flux. The search for lasers which will run at this limit is now underway.

Solid state lasers show good potential for low noise operation. Using nonplanar ring oscillator (NPRO) designs, solid-state lasers can exhibit near-ideal single-mode output [1,2]. However the intensity noise spectrum is commonly dominated by the resonant relaxation oscillation [3]. One method of controlling such intensity noise is through the use of an electronic feedback loop as shown in Fig. 1. In this scheme, some of the laser output is detected and the signal fed back out of phase to the pump source of the laser, thereby canceling some of the intensity fluctuations of the laser output. Experimentally, such systems have been demonstrated to be highly effective [4–6].

The classical theory of this control loop is well understood. Classically, the only noise input to the laser is due to the pump field. The laser behaves as a damped driven harmonic oscillator with respect to pump noise [7], and feedback to such systems is described at length in many control theory texts (see, e.g., Ref. [8]). Unfortunately this model is incomplete because it does not include quantum noise sources such as spontaneous emission, dipole fluctuations, and loss of the lasing mode. Quantum-mechanical models of electronic feedback have previously been restricted to diode lasers [9], empty cavities [10–12], intensity modulators [13] and second-harmonic generators [14].

In this work we present a quantum-mechanical model of electronic feedback to the pump source of a four-level laser. We show that the quantum-mechanical model makes significantly different predictions to the classical model. We present experimental results obtained using a Nd:YAG (yttrium aluminum garnet) NPRO, and find excellent agreement with the quantum-mechanical theory. In contrast, we find clear disagreement between the experimental results and the classical theory. We find that nonclassical behavior cannot be produced by the feedback loop, in agreement with previous work [10–13]. This is due to the amplification of anticorrelated vacuum noise by the feedback loop. This vacuum noise is introduced by the beamsplitter which directs some of the output light to the in-loop detector. By injecting a squeezed vacuum at the empty port of this beamsplitter, we show theoretically that bright squeezed light can be produced. This method of producing bright squeezing is shown to be more efficient than the passive combination of coherent light and squeezed vacuum with a beamsplitter. This scheme may be particularly suited to the production of bright squeezing at low frequencies.

The plan of the paper is as follows. In Sec. II we introduce a linearized model of the laser which includes all the quantum noise sources. An extra term to describe the feedback is introduced in Sec. III, and the equations are solved for the intensity noise spectrum. Predictions of the model for a NPRO Nd:YAG laser are presented in Sec. IV, and these results are compared to the experimental data in Sec. V. Finally, in Sec. VI we investigate the behavior of the feedback

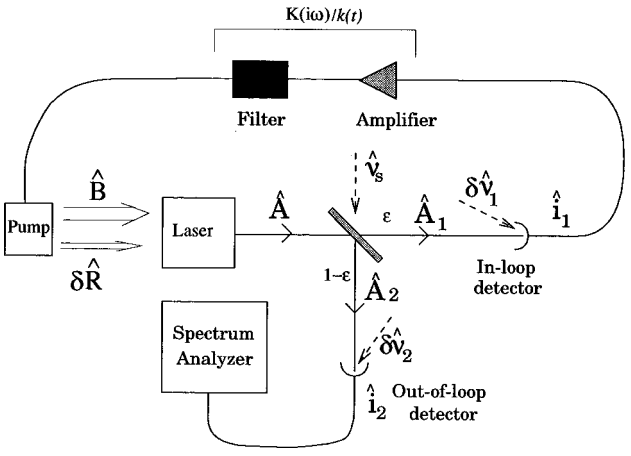

FIG. 1. The experimental setup which is modeled by the theory. The current from the in-loop detector is fed back to the pump source via a filter-amplifier circuit. The out-of-loop field is monitored on a spectrum analyzer.

loop with a squeezed vacuum at the empty port of the beam splitter.

II. LINEARIZED LASER EQUATIONS OF MOTION

Starting from the quantum Langevin equations for the four-level laser, it is possible to derive a set of linearized operator equations for the fluctuations of the atomic populations and lasing mode amplitude about their semiclassical values. Details of this derivation can be found in Refs. [15] and [16]. The equations for the linearized fluctuations, together with the steady-state semiclassical equations of motion, can be used to derive the intensity noise spectrum.

The linearized fluctuation equations are obtained by expanding the operators about their semiclassical values. For example, the operator for the laser output field $\hat{A}$ may be written as

$$\hat{A} = (\bar{A} + \delta\hat{A}) e^{\phi(t)},$$

where $\bar{A}$ is the absolute value of the semiclassical amplitude of the lasing mode, and $\delta\hat{A}$ is a zero-mean fluctuation operator. The semiclassical phase of the field is $\phi(t)$. The phase is a function of time due to the phase diffusion of the laser. The photon number operator can be written

$$\hat{n} = \hat{A}^\dagger \hat{A} \cong \bar{A}^2 + \bar{A}\,\delta\hat{X}_A,$$

where the amplitude quadrature fluctuation operator $\delta\hat{X}_A$ is defined by

$$\delta\hat{X}_A = \delta\hat{A} + \delta\hat{A}^\dagger.$$

Only terms linear in the fluctuation operators have been retained. From this discussion we can see that the variance in the photon number (i.e., the intensity noise) will be proportional to the variance of the amplitude quadrature fluctuation. In addition, the intensity noise is phase insensitive, so we can set $\phi = 0$ for all time without loss of generality.

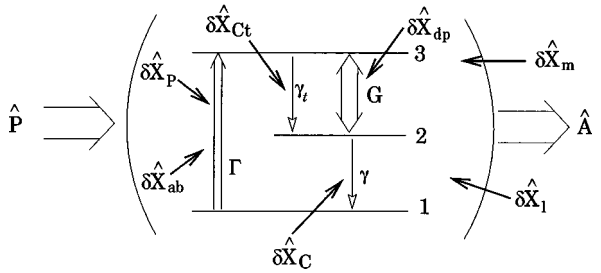

FIG. 2. A diagram of the features included in the linearized quantum model of the laser. Γ is the pump rate; γ and γ_t are spontaneous emission rates; G is the stimulated emission rate per photon; $\delta\hat{X}_C$ and $\delta\hat{X}_{Ct}$ are vacuum noise inputs due to spontaneous emission; $\delta\hat{X}_{\rm dp}$ is quantum noise due to dephasing between the lasing levels; $\delta\hat{X}_l$ is quantum noise due to internal loss; $\delta\hat{X}_m$ is quantum noise due to loss through the output mirror; $\delta\hat{X}_P$ is noise due to the pump source; and $\delta\hat{X}_{\rm ab}$ is due to inefficient pump absorption.

In addition to linearization, further simplification of the model is achieved by adiabatically eliminating the equation for the upper pump level. This leads to a unidirectional pumping of the electrons from the ground state directly to the upper lasing level. The result is a set of equations which describes a three-level laser with noise inputs as shown in Fig. 2 The electrons are pumped from the ground state to the upper lasing level at a rate Γ by the pump field $\hat{P}$. The fluctuations in the amplitude of the pump field, represented by $\delta\hat{X}_P$, introduce a source of noise into the pumping process. As not all of the pump field is absorbed, a source of quantum (or vacuum) noise, $\delta\hat{X}_{\rm ab}$, is also introduced. The lasing transition between levels 2 and 3 brings with it two sources of quantum noise: first, $\delta\hat{X}_{Ct}$ due to spontaneous emission between the lasing levels which occurs at a rate γ_t; and, second, $\delta\hat{X}_{\rm dp}$, due to dephasing of the lasing levels caused by phonon collisions. Electrons decaying out of the lower lasing level at a rate γ also give rise to a source of spontaneous emission noise, $\delta\hat{X}_C$. Other noise sources included in the model are the vacuum fluctuations $\delta\hat{X}_m$ entering the cavity through the output mirror, and $\delta\hat{X}_l$, due to other losses within the cavity. The output of the laser is the field $\hat{A}$ shown on the right of Fig. 2.

To solve for the laser spectrum we require the semiclassical equations of motion for the atomic populations and lasing mode amplitude,

$$\begin{aligned}
\dot{\alpha} &= \frac{G}{2}(J_3 - J_2)\alpha - \kappa\alpha, \\
\dot{J}_2 &= G(J_3 - J_2)\alpha^2 + \gamma_t J_3 - \gamma J_2, \\
\dot{J}_3 &= -G(J_3 - J_2)\alpha^2 - \gamma_t J_3 + \Gamma J_1, \\
J_1 + J_2 + J_3 &= 1,
\end{aligned} \tag{1}$$

where J_n is the population of level n scaled by the number of atoms N, and α is the amplitude of the lasing mode per root N. The phase of α is real since $\bar{A}$ was earlier assumed to be real. The total damping rate of the laser cavity is κ, which is the sum of the loss rate through the output mirror, κ_m, and other losses, κ_l. The rate G is the simulated emission rate per photon in the lasing mode, and is given by

$$G = \sigma_s \rho c,$$

where σ_s is the stimulated emission cross section, ρ is the density of active atoms and c is the speed of light in the lasing medium. These semiclassical equations are solved with the rate of change of the variables set to zero to find the stable steady-state operating point of the laser.

The linearized operator equations for the fluctuations of the laser parameters about their semiclassical values are [16]

$$\dot{\delta\hat{X}}_a = G(\delta\hat{\sigma}_3 - \delta\hat{\sigma}_2)\alpha + \sqrt{2\kappa_m}\,\delta\hat{X}_m + \sqrt{\kappa_l}\,\delta\hat{X}_l + \iota\sqrt{G(J_3+J_2)}\,\delta\hat{X}_{\rm dp},$$

$$\dot{\delta\hat{\sigma}}_1 = -\Gamma\sqrt{1-q}\,\delta\hat{\sigma}_1 + \gamma\delta\hat{\sigma}_2 - \sqrt{\Gamma J_1 q}\,\delta\hat{X}_P - \sqrt{\gamma J_2}\,\delta\hat{X}_C + \sqrt{\Gamma J_1(1-q)}\,\delta\hat{X}_{\rm ab}, \tag{2}$$

$$\dot{\delta\hat{\sigma}}_2 = G(\delta\hat{\sigma}_3 - \delta\hat{\sigma}_2)\alpha^2 + G(J_3 - J_2)\alpha\,\delta\hat{X}_a + \gamma_t\delta\hat{\sigma}_3 - \gamma\delta\hat{\sigma}_2 + \sqrt{\gamma J_2}\,\delta\hat{X}_C - \sqrt{\gamma_t J_3}\,\delta\hat{X}_{Ct} + \iota\sqrt{G(J_3+J_2)}\,\delta\hat{X}_{\rm dp},$$

$$\dot{\delta\hat{\sigma}}_3 = -G(\delta\hat{\sigma}_3 - \delta\hat{\sigma}_2)\alpha^2 - G(J_3 - J_2)\alpha\,\delta\hat{X}_a - \gamma_t\delta\hat{\sigma}_3 + \Gamma\sqrt{1-q}\,\delta\hat{\sigma}_1 + \sqrt{\Gamma J_1 q}\,\delta\hat{X}_P + \sqrt{\gamma_t J_3}\,\delta\hat{X}_{Ct} - \iota\sqrt{G(J_3+J_2)}\,\delta\hat{X}_{\rm dp} - \sqrt{\Gamma J_1(1-q)}\,\delta\hat{X}_{\rm ab}$$

where $\delta\hat{X}_a$ is the operator for the fluctuations of the lasing mode amplitude quadrature, $\delta\hat{\sigma}_n$ is the operator for the fluctuations of the atomic population about J_n, and the efficiency of pump absorption is given by q and $\iota = \sqrt{-1}$.

III. INCLUSION OF FEEDBACK IN THE LASER EQUATIONS

Equations (1) and (2) describe only the free-running laser. A term for feedback to the pump source must be included to model the experiment shown in Fig. 1. This is done by writing the pump field $\hat{P}$ as

$$\hat{P} = \hat{B} + \delta\hat{R}, \tag{3}$$

where $\hat{B}$ is the pump field without feedback, and $\delta\hat{R}$ is the additional field introduced by the action of the feedback. The field $\delta\hat{R}$ does not change the dc operating point of the laser, which is governed solely by $\hat{B}$. The amplitude fluctuations of the pump field may be found by linearizing $\hat{B}$ about its semiclassical value $\bar{B}$, so that

$$\begin{aligned} \hat{P} &= \bar{B} + \delta\hat{B} + \delta\hat{R} \\ &\Rightarrow \delta\hat{P} = \delta\hat{B} + \delta\hat{R} \\ &\Rightarrow \delta\hat{X}_P = \delta\hat{X}_B + \delta\hat{X}_R . \end{aligned} \tag{4}$$

The field $\delta\hat{R}$ may be expressed as a convolution of the time response of the feedback electronics, $k(t)$, and the ac component of the in-loop photocurrent, $\delta\hat{\imath}_1(t)$ [8]. For a diode pumped laser, such as the one considered in the experimental work presented in Sec. V, it can be assumed that the conversion of the feedback current into the field $\delta\hat{R}$ is independent of frequency. This is reasonable due to the large linewidth of the diode laser pump source. We will also assume that there is an optical loss β in the diode laser [17], which attenuates the feedback signal. This introduces additional vacuum noise, $\delta\hat{\nu}_f$, so that the form of the $\delta\hat{R}$ is

$$\delta\hat{R} = -\sqrt{\beta}\int_{-\infty}^{\infty} k(v)\,\delta\hat{\imath}_1(t-v)\,dv - \iota\sqrt{1-\beta}\,\delta\nu_f, \tag{5}$$

where the minus sign is included to agree with conventional notation. The amplitude quadrature fluctuation $\delta\hat{X}_R$ is then given by

$$\delta\hat{X}_R(t) = -\sqrt{\beta}\int_{-\infty}^{\infty} k(v)\,\delta\hat{X}_{i_1}(t-v)\,dv - \iota\sqrt{1-\beta}\,\delta\hat{X}_{\nu_f}. \tag{6}$$

The photocurrent $\hat{\imath}_1$ may be expressed in terms of the laser output $\hat{A}$, the beamsplitter ratio ϵ, and the detector efficiency η_1 as

$$\hat{\imath}_1 = [\sqrt{\epsilon\eta_1}\hat{A} + \iota\sqrt{\eta_1(1-\epsilon)}\,\delta\hat{\nu}_s + \iota\sqrt{1-\eta_1}\,\delta\hat{\nu}_1)^\dagger(\sqrt{\epsilon\eta_1}\hat{A} + \iota\sqrt{\eta_1(1-\epsilon)}\,\delta\hat{\nu}_s + \iota\sqrt{1-\eta_1}\,\delta\hat{\nu}_1], \tag{7}$$

where the vacuum fluctuations $\delta\hat{\nu}_s$ and $\delta\hat{\nu}_1$ are due to the beamsplitter and in-loop photodetector, respectively (see Fig. 1). The fluctuations in the current are found by linearizing Eq. (7). The field $\hat{A}$ is expanded about the semiclassical value $\bar{A}$ as $\hat{A} = \bar{A} + \delta\hat{A}$. Retaining only first-order fluctuation terms, we find that the fluctuations of the in-loop photocurrent are given by

$$\delta\hat{\imath}_1 = \sqrt{2\kappa_m}\alpha[\sqrt{\epsilon\eta_1}\,\delta\hat{X}_A + \iota\sqrt{\eta_1(1-\epsilon)}\,\delta\hat{X}_{\nu_s} + \iota\sqrt{1-\eta_1}\,\delta\hat{X}_{\nu_1}], \tag{8}$$

where we used $\bar{A} = \sqrt{2\kappa_m}\alpha$.

Equations (8), (6), and (4) can be substituted into Eqs. (2). Together with the boundary condition [18]

$$\delta\hat{X}_A = \sqrt{2\kappa_m}\,\delta\hat{X}_a - \delta\hat{X}_{Am}, \tag{9}$$

these equations may be solved in Fourier space for the amplitude quadrature fluctuations in the laser output:

$$\begin{aligned} \delta X_A = \Bigg\{ & F(\iota\omega)\left[\delta X_B + \iota\left(\frac{1-\beta}{q}\right)^{1/2}\delta X_{\nu_f}\right] + F(\iota\omega)H(\iota\omega) \\ & \times\left[\iota\left(\frac{(1-\epsilon)}{\epsilon}\right)^{1/2}\delta X_{\nu s} + \iota\left(\frac{1-\eta_1}{\epsilon\eta_1}\right)^{1/2}\delta X_{\nu_{D1}}\right] \\ & + W_1(\iota\omega)\,\delta X_m + W_2(\iota\omega)\,\delta X_C + W_3(\iota\omega)\,\delta X_{Ct} \\ & + W_4(\iota\omega)\,\delta X_{dp} + W_5(\iota\omega)\,\delta X_l \\ & + W_6(\iota\omega)\,\delta X_{ab}\Bigg\} \Big/ [1 + F(\iota\omega)H(\iota\omega)], \end{aligned} \tag{10}$$

where the form of the functions $W_n(\iota\omega)$, $H(\iota\omega)$, and $F(\iota\omega)$ are given in the Appendix. The absence of the hats over the operators in Eq. (10) indicate the Fourier transforms of the operators.

Equation (10) may be compared to the standard equation for a closed feedback loop [8]. The function $H(\iota\omega)$ may then be identified as the transfer function of the feedback system, i.e., the combined effect of the beam splitter, control electronics, and laser diode efficiency. With the sign convention chosen here, the feedback is defined as ''negative'' when Re$[H(\iota\omega)]$ is positive. Negative feedback is required to achieve noise suppression. The function $F(\iota\omega)$ is seen to be the transfer function of the free-running laser with respect to

pump noise. This is the same transfer function which may be derived from the semiclassical laser equations [7]. The functions $W_n(\imath\omega)$ are the free-running laser transfer functions for the quantum noise terms.

To calculate the noise spectrum of in- and out-of-loop fields, A_1 and A_2 respectively, we must evaluate

$$V_{A_n}=\langle|\delta X_{A_n}|^2\rangle. \tag{11}$$

The spectrum V_{A_n} is normalized by the photon flux in the field A_n, so that the QNL is given by $V_{A_n}=1$. The quadratures X_{A_n} are given in terms of X_A by

$$\delta X_{A_2}=\imath\sqrt{(1-\epsilon)}\,\delta X_A+\sqrt{\epsilon}\,\delta X_{\nu_s}, \tag{12}$$

$$\delta\hat{X}_{A_1}=\sqrt{\epsilon}\,\delta\hat{X}_A+\imath\sqrt{1-\epsilon}\,\delta\hat{X}_{\nu_s}.$$

Combining Eqs. (11), (12), and (10), the in- and out-of-loop field spectra are found to be

$$V_{A_1}=\frac{\epsilon\left[V_Q+\left|F(\imath\omega)\right|^2\left(V_B+\frac{1-\beta}{q}\right)\right]+\left|F(\imath\omega)H(\imath\omega)\right|^2\left(\frac{1-\eta_1}{\eta_1}\right)+(1-\epsilon)V_{\nu s}}{\left|1+F(\imath\omega)H(\imath\omega)\right|^2} \tag{13}$$

and

$$V_{A_2}=\frac{(1-\epsilon)\left[V_Q+\left|F(\imath\omega)\right|^2\left(V_B+\frac{1-\beta}{q}\right)+\left|F(\imath\omega)H(\imath\omega)\right|^2\left(\frac{1-\eta_1}{\eta_1\epsilon}\right)\right]+\frac{V_{\nu s}}{\epsilon}\left|\epsilon-F(\imath\omega)H(\imath\omega)\right|^2}{\left|1+F(\imath\omega)H(\imath\omega)\right|^2}, \tag{14}$$

where $V_Q=\Sigma|W_n(\imath\omega)|^2$ is the noise power due to quantum-mechanical sources within the laser, i.e. spontaneous emission, dephasing, internal loss, and loss through the output coupler; V_B is the noise of the pump source of the laser; and V_{ν_s} is the noise due to the vacuum at the beam splitter, the generality of which is maintained for work in Sec. VI.

Of most interest is the out-of-loop field, since this is the only observable output of the control loop. In the limit of no feedback [$\epsilon, H(\imath\omega)\to 0$], we find that the spectrum V_{A_2} correctly reduces to the free-running laser spectrum [15]. In the limit of large negative feedback, the out-of-loop noise is found to be

$$\lim_{H(\imath\omega)\to\infty}(V_{A2})=\frac{(1-\epsilon)(1-\eta_1)}{\eta_1\epsilon}+\frac{V_{\nu_s}}{\epsilon}. \tag{15}$$

For a Poissonian vacuum at the beam splitter ($V_{\nu_s}=1$) the high gain limit of the out-of-loop noise is always greater than 1, i.e., it is always super-Poissonian. This is in agreement with other quantum feedback models [10–13]. The cause of this behavior lies with the vacuum fluctuations introduced by the beam splitter. The noise due to the beam splitter in the out-of-loop field is out of phase with the noise introduced to the in-loop field. Negative feedback therefore amplifies the beam-splitter vacuum noise in the out-of-loop field, preventing sub-Poissonian intensity statistics.

The high gain limit of the in-loop field is found to be

$$\lim_{H(\imath\omega)\to\infty}(V_{A1})=\frac{1-\eta_1}{\eta_1}. \tag{16}$$

The noise of the in-loop field can therefore become sub-Poissonian depending on the value η_1. This is also in agreement with other quantum feedback models [10,11,13]. This field is *not* squeezed because it is not a free-field and does not obey the free field commutators.

Comparison of Eq. (14) to the semiclassical spectrum, where the only noise input is the pump noise V_B, shows that this model brings with it extra noise terms due to the lasing dynamics and the action of the beam splitter and photodetector in the feedback loop. The effect of all these extra noise inputs on the feedback control problem will now be investigated for the Nd:YAG NPRO laser.

IV. OPTIMIZATION FOR THE ND:YAG LASER

The Nd:YAG NPRO laser runs in a regime where γ is much larger than the stimulated emission rate $G\alpha^2$, the pump rate Γ, and the rate of spontaneous emission between the lasing levels, γ_t. (For values of the Nd:YAG NPRO fixed parameters, see Table I.) These assumptions permit the simplification of the pump noise transfer function to

$$F(\imath\omega)=\frac{\sqrt{2\kappa_m}\sqrt{\Gamma J_1 q}G\alpha}{\imath\omega\gamma_L+(\omega_r^2-\omega^2)}, \tag{17}$$

where

TABLE I. Parameters of the Nd:YAG laser.

Parameter	Value
κ_m	7.5×10^7 s^{-1}
κ_l	4.7×10^7 s^{-1}
γ_t	4.3×10^3 s^{-1}
γ	3.3×10^7 s^{-1}
G	6.6×10^{11} s^{-1}
q	0.9

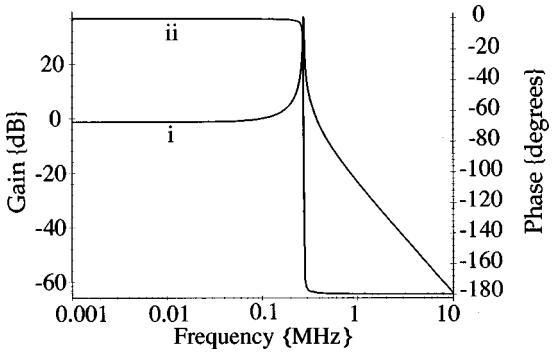

FIG. 3. A plot of the (curve i) amplitude and (curve ii) the phase of the pump noise transfer function $F(\iota\omega)$ as a function of frequency. Parameters used are those in Table I with $\Gamma=6$.

$$\omega_r=G\alpha\sqrt{J_3-J_2} \quad \text{and} \quad \gamma_L=\Gamma\sqrt{1-q}+\gamma_t+G\alpha^2.$$

Under these conditions, $F(\iota\omega)$ is seen to be a second-order transfer function, the same as could be found for a damped, driven pendulum. If the damping rate γ_L is less than ω_r, then the transfer function exhibits a resonant relaxation oscillation (RRO) [7]. A plot of the phase and amplitude of the transfer function for typical Nd:YAG parameters is shown in Fig. 3. The stabilization of a feedback loop which includes such a second order resonance is discussed at length in Ref. [8]. The goal is to ensure that the magnitude of the open-loop gain $[F(\iota\omega)H(\iota\omega)]$ is less than 1 when the phase of the open-loop gain reaches $-180°$. If this is not achieved, the feedback loop will be unstable, leading to an enhancement of the spectral noise. Note also that a stable feedback loop may amplify noise if the open-loop gain approaches -1, since the denominator of Eq. 14 approaches 0.

The Bode diagram of $F(\iota\omega)$, Fig. 3, therefore shows that we require a phase advance filter to enhance the performance of the control loop. We will consider a filter of the form

$$H_o(\iota\omega)=\lambda\frac{p+\iota\omega s^2}{p+\iota\omega}, \tag{18}$$

where the parameters s and p are chosen to refine the feedback loop. This is a simple first-order phase advance filter with dc gain λ [8]. It has a maximum phase advance of ϕ_m at frequency ω_m, where

$$\tan\phi_m=\frac{s^2-1}{2s} \quad \text{and} \quad \omega_m=\frac{p}{s}. \tag{19}$$

The amplitude response of $H_o(\iota\omega)$ is that of a high pass filter, where the attenuation ratio between low and high frequencies is s^2.

To optimize the feedback loop, the frequency ω_m is chosen to coincide with the point at which the open-loop transfer function $F(\iota\omega)H(\iota\omega)$ has a magnitude of 1 [8] by solving

$$|F(\iota\omega_m)H_o(\iota\omega_m)|=1, \tag{20}$$

$$\omega_m=\frac{p}{s}$$

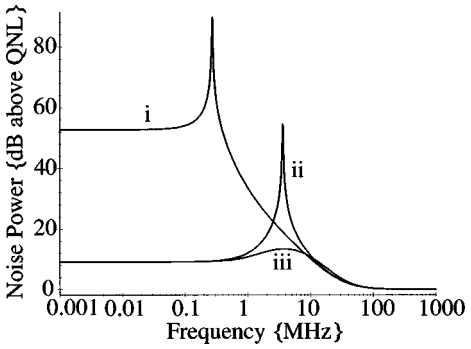

FIG. 4. The effect of feedback on the Nd:YAG spectrum: (curve i) the free-running laser spectrum, $H(\iota\omega)=0$; (curve ii) the spectrum with feedback and no phase advance filter, $H(\iota\omega)=\lambda$; and (curve iii) the spectrum with feedback and an optimized phase advance filter, $H(\iota\omega)=H_o(\iota\omega)$. Parameters used were $\Gamma=6$, $V_P=500\,000$, $\epsilon=0.5$, and $\eta_1=0.9$. The phase advance in (curve iii) is 65°, i.e., $s=4.51$.

for the parameter p. In this model we are free to choose the amount of phase advance ϕ_m, which is determined by the free parameter s.

Figure 4 shows the predicted effect of feedback on a typical Nd:YAG laser spectrum. Curve i is the free running laser spectrum, i.e., $H(\iota\omega)=0$. Curve ii is a spectrum with feedback but no phase advance filter, i.e., $H(\iota\omega)=\lambda$, where λ is a real positive number. The spectrum with the optimized phase advance filter iii shows a considerable improvement, although the spectrum still exhibits a noise peak. The origin of this peak is made clear by Fig. 5 which shows the noise spectrum split into it's various sources. Note that the noise power in this graph is on a linear scale with the QNL at 1. It demonstrates that the pump noise (curve iii) is well controlled by the feedback loop, as we would expect since the phase advance filter was designed using the pump noise transfer function. It is the sources of quantum noise arising in the laser dynamics (curves ii, iv, v, and vii) which are not well controlled by this filter. These noise sources, represented by V_Q, have a frequency dependence due to the laser

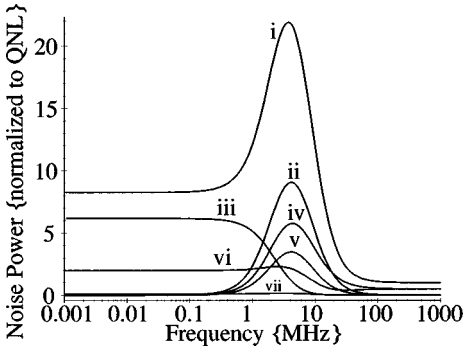

FIG. 5. The components of the spectrum with feedback. (curve i) sum of all noise terms; (curve ii) noise due to dephasing; (curve iii) pump noise; (curve iv) noise due to the output mirror; (curve v) noise due to internal loss; (curve vi) noise due to the beam splitter and in-loop detector, and (curve vii) noise due to spontaneous emission. Parameters used were $\Gamma=6$, $V_P=500\,000$, $\epsilon=0.5$, $\eta_1=0.9$, and $H(\iota\omega)=H_o(\iota\omega)$. The phase advance is 65°, i.e., $s=4.51$

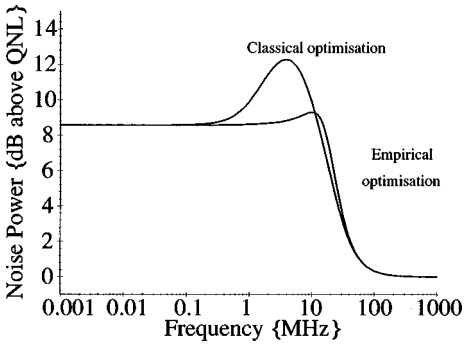

FIG. 6. The spectrum with feedback optimized using the pump noise transfer function and the improvement which can be achieved by reducing the frequency of maximum phase advance by a factor of 0.6. $\Gamma=6$, $V_P=500\,000$, $\epsilon=0.5$, and $\eta_1=0.9$. The phase advance is 65°, i.e., $s=4.51$.

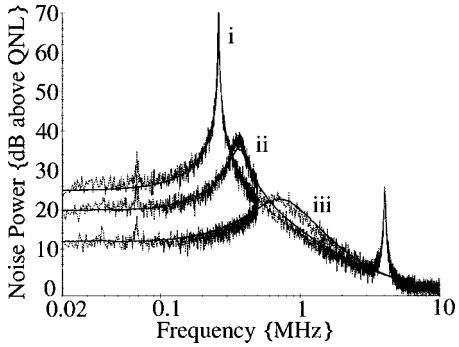

FIG. 7. Noise spectra with varying amounts of feedback: (curve *i*) free running—no feedback; (curve *ii*) feedback operational, with 20 dB of electronic attenuation in the feedback loop; (curve *iii*) feedback with no attenuation in loop, i.e., best performance of loop. The laser output power was 100 mW, of which 1 mW was detected both in and out of loop. Other parameters were $\epsilon=0.5$, $\Gamma=5.7$, $V_p=40\,000$, $\rho=0.096$, and $\tau=22$ ns.

dynamics, which is distinct from the pump noise transfer function.

The control of these noise sources can be improved empirically by reducing the frequency of the maximum phase advance, ω_m. This increases the size of $H_o(\imath\omega)$ near the resonance, thereby increasing the gain of the feedback loop at this point. The result is an improvement on the classically optimized noise suppression as shown in Fig. 6.

V. COMPARISON OF EXPERIMENT TO THEORY WITH A ND:YAG LASER

An experiment to test the theoretical predictions was set up as shown in Fig. 1. The laser used was a Nd:YAG NPRO pumped by two diode laser arrays operating at 808 nm. The maximum output power of the laser was 700 mW at 1064 nm.

The optical signals were detected using Epitax 500 InGaAs photodiodes, then amplified by a Comlinear CLC420 transimpedance amplifier. These detectors have a dynamic range >80 dB and a bandwidth from 0 to 20 MHz. The power spectrum of the signal was recorded using a Hewlett Packard HP-8568B spectrum analyzer. The detected power on each of the two detectors was $1.00(\pm 0.05)$ mW. The spectra were calibrated to the QNL by detecting 1 mW of white light illumination.

The invariant parameters of the laser, such as decay constants, are well determined, and can be found in Ref. [3]. Internal loss rates and output coupling rates are properties of the individual crystal, and have been determined by the manufacturers, *Laser Zentrum Hannover*. The pump absorption q can be estimated from the ratio of the pump field photon flux to the laser output photon flux. All these values are presented in Table I. The two remaining laser parameters, the pump noise spectrum V_P, and the pump rate Γ, are found from the free running laser spectrum. The pump rate Γ is fitted by matching the RRO frequencies of the experimental and theoretical curves. The value of Γ also determines the values of the atomic populations J_n and the photon number α^2 through the semiclassical equations of motion [Eqs. (1)]. The pump noise V_P is assumed to be frequency independent, and is fitted by matching the height of the curves at frequencies below the RRO.

A comparison of theory and experiment for the free running laser spectrum is shown by curve *i* in Fig. 7. The agreement is good, except for the peak at 4 MHz, which is due to a resonance in the current source of the laser diodes and is therefore not accounted for by the theory.

The circuit used in the feedback loop consisted of a series of active filters to provide phase advance and gain. The maximum phase advance was 36° at 800 kHz, and the maximum electronic gain in the feedback loop was 50 dB at 10 MHz. The feedback signal was ac coupled to the diode laser current source to prevent any change in the output power of the diode laser.

To fit the noise spectra with feedback requires some additional parameters. The transfer function for the feedback system is taken to be

$$H(\imath\omega)=\rho K(\imath\omega)e^{-\imath\omega\tau}, \tag{21}$$

where $K(\imath\omega)$ is the transfer function of the electronics in the feedback loop. This transfer function was measured using a Hewlett-Packard 3536A network analyzer. The parameter τ is a time delay due to the laser diodes and beam path which is not included in $K(\imath\omega)$. Time delays are important, as they introduce a phase lag which counteracts the required phase advance. This extra time delay was also measured using the network analyzer. The parameter ρ expresses the change in gain due to the detected quantities of light and the unknown efficiency of the laser diodes. The value of ρ was fitted to the noise spectrum showing the most suppression, i.e., largest feedback gain. The gain was then controlled electronically within the feedback loop using variable attenuators. The value of ρ could therefore be scaled, rather than fitted to each new spectrum. This served as a test of the consistency of this fitted parameter.

An example of the effect of the feedback loop is shown by curves *ii* and *iii* in Fig. 7. These results show good agreement between theory and experiment. The noise peak at 4 MHz is not suppressed by the feedback because it is outside the bandwidth of the system. The best noise suppression achieved with this system is shown by curve *iii*.

Theoretical investigation of the feedback system in Sec. IV showed that quantum-mechanical noise sources make an

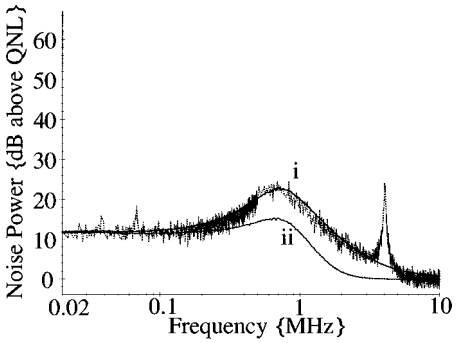

FIG. 8. The effect of quantum noise on the laser spectrum. Curve *i* shows the experimental results and theoretical model while curve *ii* shows the semiclassical model. Parameters used were $\epsilon=0.5$, $\Gamma=5.7$, $V_p=40\,000$, $\rho=0.096$, and $\tau=22$ ns.

important contribution to the noise spectrum. This is shown experimentally in Fig. 8. Curve *i* shows the experimental noise spectra and quantum-mechanical theory curve. The lower curve *ii* is the noise spectrum arising from only the pump noise, although a 1 has been added to the spectrum to account for the QNL. This is the semiclassical spectrum which may be found from the semiclassical laser equations. Figure 8 clearly shows that the semiclassical model, even allowing for the QNL, does not provide a complete description of the observed noise spectrum.

VI. NONCLASSICAL APPLICATIONS OF THE FEEDBACK LOOP

The fully quantum-mechanical nature of this model allows the investigation of feedback in regimes where lasers are predicted to produce nonclassical light. It has been shown [19] that a laser pumped by an amplitude-squeezed source can itself produce amplitude squeezed light. The Nd:YAG laser is predicted to generate amplitude squeezing at low frequencies when pumped by a broadband squeezed diode laser [15]. At higher frequencies the squeezing is swamped by the RRO. The question then arises as to whether feedback may be employed to damp the RRO and preserve low-frequency amplitude squeezing. Unfortunately, suppressing the RRO requires large amounts of negative feedback. The vacuum noise due to the beamsplitter is therefore amplified by the feedback loop, hence destroying squeezing at low frequencies.

Lasers are also predicted to generate amplitude squeezed light at the *rate-matched* condition [20,22]. If this condition occurs too close to threshold, however, the squeezing is destroyed by excess spontaneous emission noise. As before, feedback cannot be used to damp this noise and recover amplitude squeezing due to vacuum noise introduced by the beam splitter.

Generating bright squeezed light

It has been suggested by many authors [9–11,13] that quantum nondemolition (QND) measurements may be used to extract an amplitude squeezed beam from the in-loop field. Previous suggestions for a QND measurement of the in-loop field have involved the use of nonlinear optical materials such as Kerr media [9,10]. One promising QND

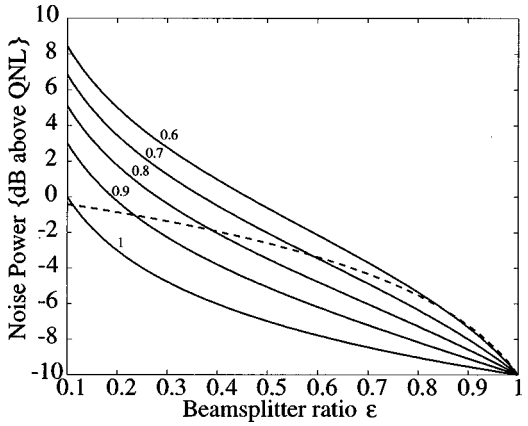

FIG. 9. A plot of bright squeezing achievable with feedback as a function of the beamsplitter ratio, ϵ. The bright squeezing in the out-of-loop field using a feedback loop running in the high gain limit with a 10-dB squeezed vacuum incident on the beam splitter is shown by the solid curves for different values of the in-loop detection efficiency. The dashed line is the bright squeezing obtained by beating a coherent source with a 10-dB squeezed vacuum.

scheme, which was demonstrated experimentally by Bruckmeier *et al.* [21], is the use of a squeezed vacuum state incident on a beam splitter. A squeezed vacuum incident on the beam splitter in the feedback loop can be included in our model by altering V_{ν_s}. Equations (16) and (15) show that for a 50/50 beam splitter ($\epsilon=0.5$) reducing V_{ν_s} will make V_{A1} and V_{A2} identical. A squeezed vacuum can therefore be used to make a QND measurement of the in-loop field.

This scheme can be used as an efficient means of converting a squeezed vacuum into a bright squeezed field. Figure 9 shows the high gain limit of the out-of-loop field [given by Eq. (15)] with a 10-dB squeezed vacuum injected on the beamsplitter. The dashed line shows the bright squeezing obtained by beating a 10-dB squeezed vacuum with a coherent field at a beam splitter. The graph clearly shows the increased transfer of squeezing to the out-of-loop field with feedback compared to that achieved by simply beating the vacuum with a coherent source. It also shows the critical dependence of the achievable squeezing on the efficiency of the in-loop photodetector. Any form of in-loop attenuation will have a similar effect on the performance of this system.

The spectrum of the out-of-loop field with a 10-dB squeezed vacuum incident on the beam splitter ($\epsilon=0.5$) is shown in Fig. 10. As the gain is increased in the feedback loop, the amount of bright squeezing on the output is increased to a maximum of 6 dB below the QNL. Significantly, the maximum bright squeezing is achieved at low frequencies. This is in contrast to most bright squeezed sources (such as second-harmonic generators) in which the bright squeezing at low frequencies is obscured by excess laser noise. In this system the feedback loop is running in the regime of large negative feedback, so that all laser noise is damped.

The dashed line at 2.6 dB below the QNL shows the bright squeezing obtained by beating a coherent source with a 10-dB squeezed vacuum at a 50/50 beam splitter. An experimental realization of this result requires a laser which is shot-noise limited at low frequencies. Even if such a laser were available, the output squeezing is still less than that

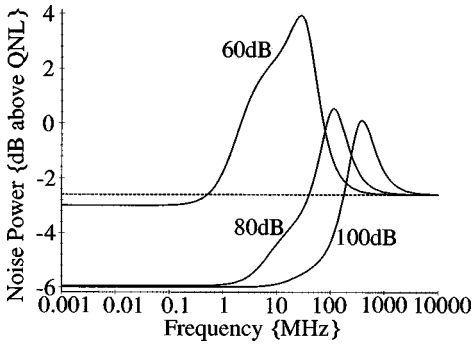

FIG. 10. Plots of the out-of-loop field spectrum showing the effect of a 10-dB squeezed vacuum incident on the beam splitter with $\epsilon = 0.5$. The efficiency of the in-loop detection system is taken to be 0.95. The dashed line shows the squeezing obtained by beating a coherent field with a 10-dB squeezed vacuum at a 50/50 beam splitter. Other parameters were $\Gamma = 6$, $V_P = 500\,000$, and $H(\iota\omega) = H_o(\iota\omega)$, with $s = 4.51$.

achievable with a feedback system.

The best currently achievable vacuum squeezing is 7.8 dB below the QNL [23] using an optical parametric oscillator (OPO). These devices require substantial amounts of pump power at twice the frequency of the output squeezed vacuum. Furthermore, a well-defined phase relationship is required between the bright light in the feedback loop and the vacuum squeezing. A possible experimental setup to extract bright squeezing using feedback is shown in Fig. 11. Here, the master laser of an injection locking system provides the power for the SHG-OPO system and locks the phase of the slave which is incorporated in the feedback loop. Injection locking alters the dynamics of the slave laser, so that the above theory is not directly applicable to an injection-locked laser. More detailed calculations show, however, that the maximum bright squeezing predicted by Eq. (14), and the frequency regime in which it occurs, remain unchanged by injection locking.

VII. CONCLUSION

The behavior of a four-level laser with electronic feedback to the pump source has been investigated both theoretically and experimentally. The theoretical model was derived using a linearized system of quantum Langevin equations which included a pump field modified by the feedback.

It was shown for the Nd:YAG laser that quantum noise due to the lasing dynamics is important when optimizing the feedback loop. A classical optimization which considers only the pump noise transfer function ignores quantum noise sources which have a unique frequency dependence. The experimental results obtained with a Nd:YAG laser show good agreement with theory. In particular, the importance of quantum noise in the laser spectrum has been clearly demonstrated.

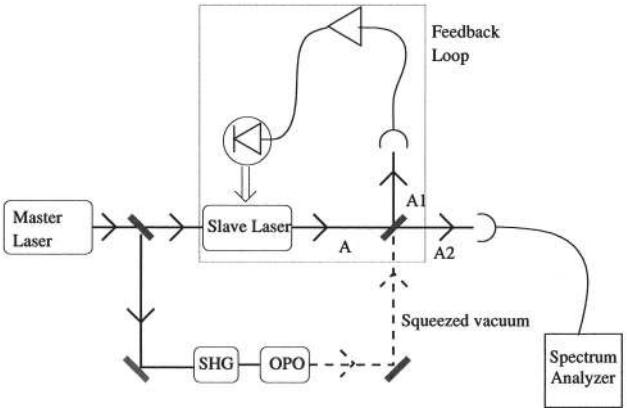

FIG. 11. An experimental setup which could be used to generate bright squeezed light with a feedback loop.

When running in a negative feedback configuration, as required to damp classical noise, this type of system was shown to destroy sub-Poissonian intensity statistics. This arises from vacuum noise due to the beam splitter, which introduces anticorrelated noise in and out of the loop.

A scheme in which the feedback loop can act as an efficient means of converting vacuum squeezing into bright squeezed light was also discussed. By using the squeezed vacuum to make a QND measurement of the in-loop field, the out-of-loop field can become highly squeezed. This method has the advantage that the resulting bright beam is sub-Poissonian at low frequencies, where bright squeezing is often destroyed by excess laser noise. Implementation of this idea may involve an injection locking system to provide sufficient power to run a squeezed vacuum generator.

ACKNOWLEDGMENTS

We wish to thank M. B. Gray, H.-A. Bachor, D. E. McCelland, and G. Dickens for many productive discussions. This work was supported by the Australian Research Council.

APPENDIX

Definition of the functions appearing in Eq. (10).

$$F(\iota\omega) = \frac{G\alpha\sqrt{2\kappa_m}\sqrt{J_1\Gamma q}(\iota\omega + \gamma - \gamma_t)}{\iota\omega\zeta(\iota\omega) + G^2\alpha^2(J_3 - J_2)(2\Gamma\sqrt{1-q} + 2\iota\omega + \gamma)}, \tag{A1}$$

$$H(\iota\omega) = 2\sqrt{\beta}\eta_1\epsilon\alpha\sqrt{2\kappa_m}K(\iota\omega), \tag{A2}$$

$$W_1(\iota\omega) = \frac{2\kappa_m\zeta(\iota\omega)}{\iota\omega\zeta(\iota\omega) + G^2\alpha^2(J_3 - J_2)(2\Gamma\sqrt{1-q} + 2\iota\omega + \gamma)} - 1, \tag{A3}$$

$$W_2(\imath\omega) = -\frac{G\alpha\sqrt{2\kappa_m\gamma J_2}(\gamma_t 2\Gamma\sqrt{1-q}+\imath\omega)}{\imath\omega\zeta(\imath\omega)+G^2\alpha^2(J_3-J_2)(2\Gamma\sqrt{1-q}+2\imath\omega+\gamma)}, \tag{A4}$$

$$W_3(\imath\omega) = \frac{G\alpha\sqrt{2\kappa_m\gamma J_3}(2\Gamma\sqrt{1-q}+2\imath\omega+\gamma)}{\imath\omega\zeta(\imath\omega)+G^2\alpha^2(J_3-J_2)(2\Gamma\sqrt{1-q}+2\imath\omega+\gamma)}, \tag{A5}$$

$$W_4(\imath\omega) = -\frac{\imath\sqrt{2\kappa_m G(J_3+J_2)}G\alpha^2(2\Gamma\sqrt{1-q}+2\imath\omega+\gamma)-\zeta(\imath\omega)}{\imath\omega\zeta(\imath\omega)+G^2\alpha^2(J_3-J_2)(2\Gamma\sqrt{1-q}+2\imath\omega+\gamma)}, \tag{A6}$$

$$W_5(\imath\omega) = \frac{2\sqrt{\kappa_m\kappa_l}\zeta(\imath\omega)}{\imath\omega\zeta(\imath\omega)+G^2\alpha^2(J_3-J_2)(2\Gamma\sqrt{1-q}+2\imath\omega+\gamma)}, \tag{A7}$$

$$W_6(\imath\omega) = \left(\frac{1-q}{q}\right)^{1/2} F(\imath\omega), \tag{A8}$$

$$\zeta(\imath\omega) = (\imath\omega+2G\alpha^2+\gamma+\gamma_t)(\Gamma\sqrt{1-q}+\imath\omega)+(G\alpha^2+\gamma_t)\gamma. \tag{A9}$$

[1] T. J. Kane and R. L. Byer, Opt. Lett. **10**, 65 (1985).
[2] A. C. Nilsson, E. K. Gustafson, and R. L. Byer, IEEE J. Quantum Electron. **25**, 676 (1989).
[3] W. Koechner, *Solid-State Laser Engineering*, 5th ed. (Springer, New York, 1996).
[4] T. J. Kane, IEEE Photonics Technol. Lett. **2**, 244 (1990).
[5] S. Rowan, A. M. Campbell, K. Skeldon, and J. Hough, J. Mod. Opt. **41**, 1263 (1994).
[6] C. C. Harb, M. B Gray, H.-A. Bachor, R. Schilling, P. Rottengatter, I. Freitag, and H. Welling, IEEE J. Quantum Electron. **30**, 2907 (1994).
[7] A. Yariv, *Optical Electronics*, 4th ed. (Saunders, Orlando, 1991).
[8] R. C. Dorf and R. H. Bishop, *Modern Control Systems*, 7th ed. (Addison-Wesley, Reading, MA, 1995).
[9] Y. Yamamoto, N. Imoto, and S. Machida, Phys. Rev. A **33**, 3243 (1986).
[10] H. A. Haus and Y. Yamamoto, Phys. Rev. A **34**, 270 (1986).
[11] H. M. Wiseman and G. J. Milburn, Phys. Rev. A **49**, 1350 (1994).
[12] H. M. Wiseman, Phys. Rev. A **49**, 2133 (1994).
[13] M. S. Taubman, Ph.D. thesis, Australian National University, Canberra, Australia, 1995.
[14] H. M. Wiseman, M. S. Taubman, and H.-A. Bachor, Phys. Rev. A **51**, 3227 (1995).
[15] T. C. Ralph, C. C. Harb, and H.-A. Bachor, Phys. Rev. A **54**, 4359 (1996).
[16] T. C. Ralph, Phys. Rev. A **55**, 2526 (1997).
[17] D. C. Kilper, D. G. Steel, R. Craig, and D. R. Scifres, Opt. Lett. **21**, 1283 (1996).
[18] C. W. Gardiner and M. J. Collett, Phys. Rev. A **31**, 3761 (1985).
[19] Y. Yamamoto, S. Machida, and A. C. Nilsson, Phys. Rev. A **34**, 4025 (1986).
[20] H. Ritsch, P. Zoller, C. W. Gardiner, and D. F. Walls, Phys. Rev. A **44**, 3361 (1991).
[21] R. Bruckmeier, H. Hanson, K. Schneider, S. Schiller, and J. Mlynek, Phys. Rev. Lett. **79**, 23 (1996).
[22] T. C. Ralph and C. M. Savage, Quantum Opt. **5**, 113 (1993).
[23] G. Breitenbach, T. Müller, S. F. Pereira, J.-Ph. Poizat, S. Schiller, and J. Mlynek, J. Opt. Soc. Am. B **12**, 2364 (1995).